Hollow agarose microneedle with silver coating for intradermal surface-enhanced Raman measurements : a skin-mimicking phantom study

Yuen, Clement; Liu, Quan

2015

Yuen, C., & Liu, Q. (2015). Hollow agarose microneedle with silver coating for intradermal surface-enhanced Raman measurements : a skin-mimicking phantom study. Journal of biomedical optics, 20(6), 061102-.

https://hdl.handle.net/10356/106904

https://doi.org/10.1117/1.JBO.20.6.061102

Journal of Biomedical Optics

BiomedicalOptics.SPIEDigitalLibrary.org

Hollow agarose microneedle with silver coating for intradermal surface-enhanced Raman measurements: a skin-mimicking phantom study

Clement Yuen
Quan Liu

SPIE.

Hollow agarose microneedle with silver coating for intradermal surface-enhanced Raman measurements: a skin-mimicking phantom study

Clement Yuen and Quan Liu*
Nanyang Technological University, School of Chemical and Biomedical Engineering, Division of Bioengineering, 70 Nanyang Drive, Singapore 637457, Singapore

Abstract. Human intradermal components contain important clinical information beneficial to the field of immunology and disease diagnosis. Although microneedles have shown great potential to act as probes to break the human skin barrier for the minimally invasive measurement of intradermal components, metal microneedles that include stainless steel could cause the following problems: (1) sharp waste production, and (2) contamination due to reuse of microneedles especially in developing regions. In this study, we fabricate agarose microneedles coated with a layer of silver (Ag) and demonstrate their use as a probe for the realization of intradermal surface-enhanced Raman scattering measurements in a set of skin-mimicking phantoms. The Ag-coated agarose microneedle quantifies a range of glucose concentrations from 5 to 150 mM inside the skin phantoms with a root-mean-square error of 5.1 mM within 10 s. The needle is found enlarged by 53.9% after another 6 min inside the phantom. The shape-changing capability of this agarose microneedle ensures that the reuse of these microneedles is impossible, thus avoiding sharp waste production and preventing needle contamination, which shows the great potential for safe and effective needle-based measurements. [DOI: 10.1117/1.JBO.20.6.061102]

Keywords: Raman spectroscopy; surface plasmons; sensors; plasmonics; biomedical optics; materials.

Paper 140380SSR received Jun. 14, 2014; revised manuscript received Aug. 25, 2014; accepted for publication Sep. 11, 2014; published online Feb. 20, 2015.

1 Introduction

Microneedles show great potential for easy administration by any layperson in the application of drug delivery[1] and blood sampling[2] of the human intradermal skin layer. Since these metal microneedles penetrate the human skin barrier, important information from the intradermal skin layer could be obtained by using these microneedles as measurement probes, for example, checking the capillary blood sugar level[3] for diabetes diagnosis or the presence of antigens in T cells[4] for immunity surveillance. These components are mainly found in the dermis layer below the skin epidermis layer, which has a thickness of few tens of micrometers up to 500 μm for our finger tips, facial, or palm skin.[5] Different techniques[6] which employ the microneedle as a measurement probe are possible, such as fluorescence, confocal microscopy, and Raman spectroscopy. Among these methods, Raman spectroscopy provides more chemical information and specific molecular chemical fingerprints,[7] but at the cost of having difficulty probing into this depth[8] and the Raman signal of the endogenous biomolecules is weak.[9] To overcome these shortcomings, surface-enhanced Raman scattering (SERS) has shown a potential to achieve larger penetration depths with augmented signals.[9–11] We have demonstrated using a stainless steel microneedle coated with a silver (Ag) film as a measurement probe for *in situ* SERS measurements using stainless steel microneedles in a skin phantom study.[12] However, the wide use of these metal and stainless steel needles[3,11,12] would yield sharp waste and the potential reuse of microneedles without adequate sterilization.[13] The typical dissolvable microneedle[1] employed to prevent sharp waste could not solve this issue, since these dissolvable microneedles are solid without any lumen and are difficult to be used as a probe after being dissolved.

Recently, an agarose microneedle adhesive has been demonstrated to effectively penetrate and swell to mechanically interlock the tissue in skin grafting.[14] This shape-changing capability of agarose after insertion into the muscle tissue for more than 2 min could be exploited in our microneedle-based intradermal SERS measurements. In this work, we propose a hollow agarose microneedle with an Ag coating for SERS detection of crystal violet (CV) and glucose test molecules embedded at a depth larger than 700 μm underneath the skin phantom surface. This agarose microneedle can achieve a sensitivity of glucose detection comparable with the previously reported stainless steel microneedles and keep all the advantages stated earlier. In addition, this new needle possesses the following additional advantages compared with the stainless steel microneedles for intradermal measurements: (1) the tip of the microneedle will be bent after exposed to water in measurements thus preventing sharp waste and potential reuses or contamination from reuses; (2) the agarose material would be more biocompatible than stainless steel even if the microneedle was broken inside the skin; and (3) the microneedle is cost effective thus suitable for use in developing regions. The original facile fabrication procedure for these SERS agarose microneedles is described. Finally, the ability of this disposable agarose microneedle to prevent sharp waste production after usage and reuse of the microneedle is investigated.

*Address all correspondence to: Quan Liu, E-mail: quanliu@ntu.edu.sg

1083-3668/2015/$25.00

2 Materials and Methods

2.1 *Chemicals and Reagents*

Silver nitrate ($AgNO_3$) and sodium hydroxide pellets were purchased from Merck, Darmstadt, Germany. D-Glucose anhydrous, CV, 1-decnaethiol, and 28% ammonium hydroxide (NH_4OH) were ordered from Alfa Aesar, Ward Hill, Massachusetts. Agarose powder was purchased from Vivantis, Selangor, Malaysia. Nigrosin (Nigrosin water soluble) and 20% intralipid were obtained from Sigma Aldrich, St. Louis, Missouri. All chemicals used were of the analytical grade.

2.2 *Fabrication of Ag-Coated Agarose Microneedle*

Figure 1 shows the steps in the Ag-coated agarose microneedle fabrication. Six percent of the agarose was boiled with 50 ml of deionized water in a microwave oven [R369T(S), Sharp, Osaka, Japan]. Figure 1(a) shows that the agarose solution was drawn up into a pipette tip (1000-μl Pipet tip, T-1000-B, Axygen, Corning, New York) with an acupuncture needle of diameter 200 μm (0.2 mm $\times$ 40 mm acupuncture needle, Beng Kang Import & Export, Woodlands, Singapore) held in a fixed position inside the tip. In this experiment, the pipette tip and the acupuncture needle act as the microneedle mold and the axial rod for creating the lumen, respectively. The fixed agarose and acupuncture needle was subsequently removed from the pipette tip [Fig. 1(b)], which was further dried naturally for another 18 h [Fig. 1(c)]. The acupuncture needle was removed to leave behind a hollow agarose tube [Fig. 1(d)] prior to the coating of a layer of silver film onto the agarose tube. This Ag layer was coated by using Tollen's method to form a SERS-active film, since we have shown that a silver coating on our stainless steel microneedle synthesized by this technique[12] provides effective augmentation in Raman signals. These parameters were selected in the Tollen's process to fabricate the Ag coating because the Ag layer coating is shown to produce surface topographies, such as surface roughness, for effective SERS enhancement at the 785-nm excitation wavelength based on our simulation in our previous publication[12] on fabrication of the Ag-coated stainless steel microneedles. During the Raman measurement, the density of silver nanoparticles on the swollen agarose microneedles should be comparable with that obtained at the end of the Tollen's procedure, since the agarose microneedles were also swollen during this Ag-coating process. Briefly, the agarose tube was dipped into 1.5 ml of 0.5 M $AgNO_3$, mixed with 0.75 ml of 2.5 M NaOH. A 0.2 ml of NH_4OH was subsequently introduced into the aforesaid solution to redissolve the precipitates, followed by the reduction of Ag ions into Ag through the addition of 4.5 ml of 0.1 M glucose solution. The agarose tube was removed from the mixture after 15 min and washed with deionized water. Then, the acupuncture needle was inserted back into the same hole for drying. Subsequently, the Ag-coated agarose microneedle was cut by a razor sharp blade to create a beveled angle at 15 ± 5 deg for the tip [Fig. 1(e)] and into a total length of about 2 mm $\pm$ 200 μm (variation in bevel angles and length was obtained in five different samples). Prior to glucose measurements, the Ag-coated agarose microneedle was soaked in 1-decanethiol at a concentration of 1 mM in ethanol for 12 h. The soaking procedure of 1-decanethiol was skipped for the Ag-coated agarose microneedle used in the SERS measurements of CV. 1-Decanethiol was used to coat the Ag-coated agarose microneedles for glucose detection, since this layer of 1-decanethiol molecules (see Appendix)[15] could capture and enrich the concentrations of glucose molecules in close vicinity to the Ag nanoparticles.

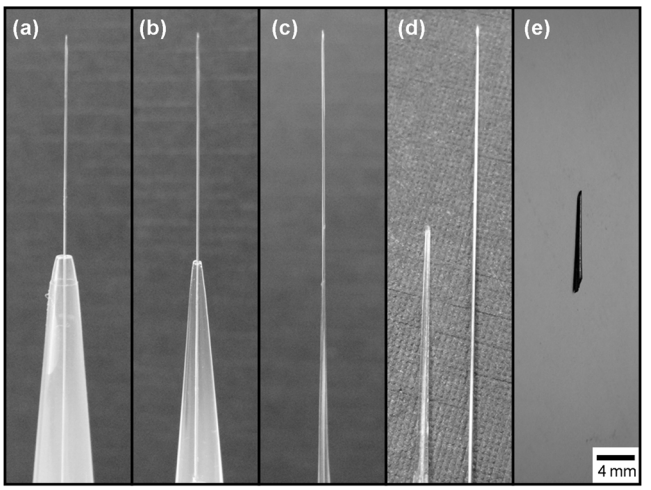

Fig. 1 Agarose microneedle fabrication steps: (a) agarose in pipette with acupuncture needle, (b) agarose and acupuncture needle removed from pipette, (c) dried for 18 h, (d) agarose microneedle removed from acupuncture needle, and (e) final Ag-coated agarose microneedle. The scale bar is shared by all figures.

2.3 *Synthesis of Skin-Mimicking Phantom*

The design and synthesis procedures of the skin-mimicking phantom were reported in our previous work[12] and are briefly summarized below. A 1% agarose solution was boiled in the microwave oven and cooled to 60°C prior to the addition of 6 μM of nigrosin and 1.967 ml of intralipid-20% to form a phantom mixture with a total volume of 50 ml. The nigrosin and intralipid were introduced to modify the optical absorption and scattering properties, respectively, of the phantom to mimic those of the human skin. The phantom mimicking the epidermis of the skin was fabricated by fixing the agarose phantom between two glass slides, which were spaced 760 μm from each other by stacking four cover slips. This 760-μm layer was stacked on top of another phantom layer mimicking the dermis, which was introduced with test molecules. These test molecules included CV (10^{-2} to 10^{-6} M) to represent chemicals in general and glucose (0 to 150 mM) to represent biomolecules, which were introduced into the aforesaid phantom mixture at 60°C at a range of concentrations inside a Petri dish for fixing. Thus, the phantom design enabled the evaluation of the Ag-coated agarose microneedle in the penetration of the 760-μm layer to sensitively detect test molecules in the deeper layer.

2.4 *Raman Measurements*

We characterized the SERS performance of the Ag-coated agarose microneedle in the skin-mimicking phantom as reported previously[12] with a micro-Raman system setup (Fig. 2, inVia, Renishaw, Gloucestershire, UK) based on a backscattering-geometry microscope (Alpha 300, WITec, Ulm, Germany). The fabricated Ag-coated agarose microneedle was perpendicular through the 760-μm layer into the layer with test molecules in

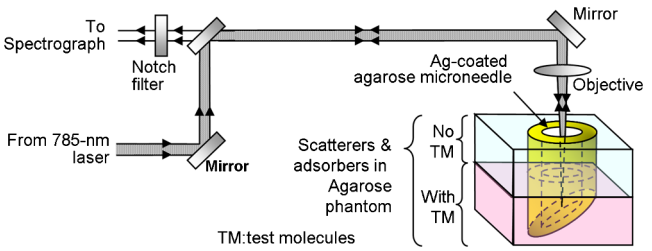

Fig. 2 Schematic of the Raman setup for SERS measurements using a microneedle.

the skin-mimicking phantom. A microscope objective (20×, NA = 0.4, Leica, Solms, Germany) was employed to focus a 785-nm laser (Renishaw) light at about 675 μm below the surface of the top layer, which was identified as the optimal position to achieve a maximum SERS signal intensity,[12] into the lumen of the Ag-coated agarose microneedle. An excitation power of 5 mW was employed for the SERS measurements and 100 mW was used in ordinary Raman measurements with and without the agarose microneedle. The microneedle went through the 760-μm phantom layer and reached the test molecules embedded in the deeper phantom layer. Emitted SERS signals that propagated in the opposite direction were collected and analyzed. Each raw spectrum was acquired with an integration time of 10 s and a spectral resolution of 2 cm^{-1}. These raw data were baseline corrected and smoothed to reduce the noise by using a five-point moving average prior to the removal of fluorescence background to yield the spectra shown in subsequent figures. The final CV and glucose spectra shown were averaged from five different samples with a standard deviation of less than 5% and 10%, respectively.

2.5 *Field Emission Scanning Electronic Microscope Analysis*

We studied the surface morphologies of the agarose microneedle with and without an Ag coating as well as the 1-decanethiol-modified Ag surface by the field emission scanning electronic microscope (FESEM) (JOEL JSM-6700F, JOEL, Tokyo, Japan) system at an accelerating voltage of 5 kV. A fine coater (JOEL JFC-1600, JOEL, Tokyo, Japan) was used to coat a thin layer of platinum onto all samples prior to the FESEM examination.

3 Results and Discussion

3.1 *Fabrication Methodology and Geometrical Topography of the Agarose Microneedle*

Figure 3 gives the representative FESEM images of the Ag-coated agarose microneedle. These Ag-coated agarose microneedles have a diameter of about 400 ± 50 μm at the tip with a bevel angle of about 15 ± 5 deg (variations in diameters and bevel angles obtained in five different samples) [Fig. 3(a)], since this angle has shown good mechanical strength for effective penetration[2] in metal microneedles. The lumen of this microneedle conforms to the size of the acupuncture needle with a diameter of 200 μm that has been used as an axial rod structure. Figure 3(b) illustrates that the agarose surface is smooth and nonporous without the Ag coating. This flat topography is attributed to the high percentage of agarose used and 18-h drying, in which the interestingly prolonged drying process has also been employed in agarose lamellar scaffolds for

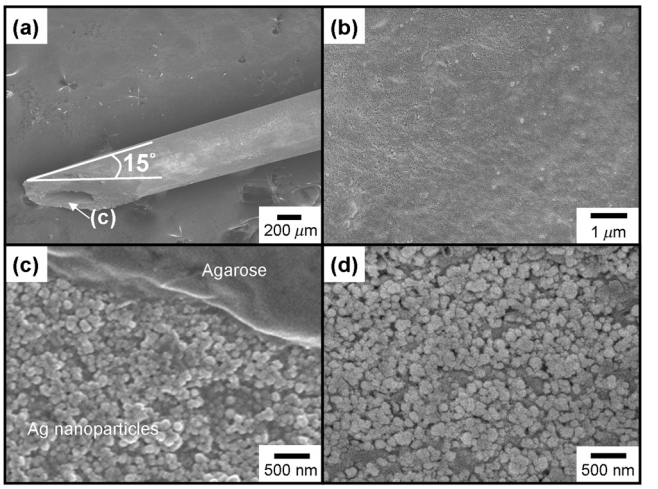

Fig. 3 Field emission scanning electronic microscope (FESEM) images of (a) Ag-coated agarose microneedle, (b) agarose microneedle without Ag coating, (c) inside the lumen at the tip of the Ag-coated agarose microneedle, and (d) Ag-coated agarose microneedle modified with 1-decanethiol.

other applications[16] such as drug delivery. Figure 3(c) demonstrates the formation of Ag nanoparticles on the wall inside the lumen of the agarose microneedle coated using the Tollen's method. The uncoated agarose corresponds to a slanted cutting interface that is created from the realization of the bevel tip after the Tollen's procedure. The Ag nanoparticles can be coated as long as about 1.5 cm into the lumen from the tip of the microneedle to facilitate SERS activities, beyond which the density of the Ag nanoparticles decreases. These surface roughness and gaps formed by the Ag nanoparticles are minimally modified [Fig. 3(d)] by the self-assembled monolayer, 1-decanethiol, for effective SERS detection of glucose molecules.

These microneedles fabrication procedures are facile and independent of complicated steps and expensive equipment, such as photolithography machines, and the clean room requirement,[17] which are typically required in the fabrication of microneedles. Since the diameter of the intermediate microneedle replica [Fig. 1(b)] is relatively much larger than that of the final microneedle [Fig. 1(d)], the microneedle mold could be easily realized by the available three-dimensional printing[18] techniques, rather than the employment of specialized techniques[17] (e.g., photography) to create the mold. Hence, the aforesaid factors allow the cost effective mass production of these hollow agarose microneedles.

3.2 *Chemical Analysis of CV in Skin Phantom*

To access the functionality of the agarose microneedle as a probe for SERS measurements, we compare (a) the SERS spectra of CV by using the Ag-coated agarose microneedle, the ordinary Raman of CV (b) by using an agarose microneedle without coating, and (c) without any microneedle to probe into the two-layered skin phantom (Fig. 4). Prominent Raman peaks including the dimethylamino groups (726 cm^{-1}), the out-of-plane C—H bend (806 cm^{-1}), the ring breathing mode (914 cm^{-1}), the in-plane aromatic C—H bending modes (1176 cm^{-1}), the in-plane C—H bending mode (1368 cm^{-1}), the symmetrical N—C—ring—C—C stretching mode (1387 cm^{-1}), and the out-of-phase ring stretch (1587 and 1621 cm^{-1})[19] are noted in the SERS spectra [Fig. 4(a)]. In particular, the enhanced

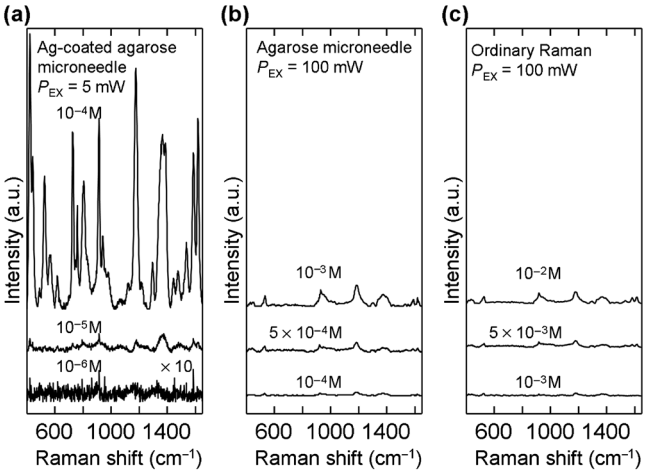

Fig. 4 Surface-enhanced Raman scattering (SERS) spectra of crystal violet (CV) molecules positioned inside phantom at 760 μm below the surface measured by using (a) Ag-coated agarose microneedle (CV concentrations: 10^{-4}, 10^{-5}, and 10^{-6} M; P_{EX}:5 mW), (b) agarose microneedle without coating (CV concentrations: 10^{-3}, 5×10^{-4}, and 10^{-4} M; P_{EX}:100 mW), and (c) without any microneedle (CV concentrations: 10^{-2}, 5×10^{-3}, and 10^{-3} M; P_{EX}:100 mW). P_{EX} means the excitation power.

peaks at 1176, 1368, and 1387 cm^{-1} are the signature peaks noted in the SERS spectra of CV[19] which are difficult to see in the ordinary Raman spectra of CV [Figs. 4(b) and 4(c)]. Moreover, the ordinary Raman spectra show weak signal intensities, despite the higher CV concentrations of more than 10^{-3} M and larger excitation power of 100 mW.

We compare the analytical enhancement factor (AEF) of this agarose microneedle with ($AEF_{ag\text{-}agarose}$) and without ($AEF_{agarose}$) Ag coating to that of the stainless steel microneedle with ($AEF_{ag\text{-}steel}$) and without (AEF_{steel}) Ag coating.[12] $AEF_{ag\text{-}agarose}$ and $AEF_{agarose}$ are calculated by the following equation, i.e., $I_{1176}/(P\times C)$, where P, C, and I_{1176} are the ratios of the excitation power, CV concentrations, and Raman peak intensity at 1176 cm^{-1} in the measurements using the agarose microneedle with or without Ag coating, to those of the ordinary Raman measurement without using any microneedle, respectively.[12] In the evaluation of the AEF, the excitation power employed in the SERS and ordinary Raman measurements is different. We minimize the laser excitation power at 5 mW in the SERS measurements to avoid introducing the thermal effect into the sample, which could degrade the SERS activities and signals. On the other hand, we employ a laser power of 100 mW in the ordinary Raman measurements which results in observable Raman peaks for AEF evaluation [Figs. 4(b) and 4(c)], since measurements it would be difficult to detect decent Raman signals at a lower laser excitation power without the Ag coating. The value of $AEF_{ag\text{-}agarose}$ is about 1.1×10^4 and is comparable with that of $AEF_{ag\text{-}steel}$ (2×10^4) and the enhancement factors (around 10^2 to 10^5) observed in Ag film on copper foil performed by another group[20] for chemical sensing. The variation in the AEF between the two types of microneedles could be attributed to differences in the Ag nanoparticle sizes and morphologies (Fig. 3), which is the result of the dissimilar substrate properties, e.g., charge transfer and surface roughness observed in metal nanoparticle formation,[21] for agarose and stainless steel. Moreover, the AEF_{steel} is 40, which is higher than the $AEF_{agarose}$ of 10, which can be attributed to the fact that the stainless steel has a larger lumen area of about 0.04 mm^2 than that of 0.03 mm^2 in the agarose microneedle. Therefore, these results demonstrate the feasibility of detecting chemical variations deep inside the phantom by using the Ag-coated agarose microneedle.

3.3 *Biomolecules Quantification of Glucose in Skin Phantom*

We also demonstrate the ability of the Ag-coated agarose microneedle for SERS measurements of bioanalyte molecules—glucose in the skin phantoms, as given in Fig. 5. The Raman intensities of the characteristic glucose peaks at 1076 cm^{-1} (C—C stretching), 1020 cm^{-1}, 1124 cm^{-1} (C—O—H deformation) rise proportionally with the increase in glucose concentration [Fig. 5(a)]. Other Raman peaks at 714, 889, 999, 1073, and 1128 cm^{-1} that are observed in the spectra are contributed by the 1-decanethiol layer on the Ag coating;[15] thus the corresponding Raman intensities are independent of glucose concentration.

Then the glucose concentrations inside the skin phantoms were estimated for all acquired 50 sets of data using the partial least square (PLS) regression and a leave-one-out (LOO) method,[12] as shown in Fig. 5(b). In every dataset, the background of 1-decanethiol was subtracted from the characteristic glucose Raman peak [for example, in 1124 cm^{-1}, C—O—H deformation was subtracted by the background of 1-decanethiol to obtain the area under this Raman peak for a full-width at half-maximum (FWHM) of 10 cm^{-1}]. Thus, we obtain the estimated glucose concentration ($C_{est,n}$, where $n = 1,2,\ldots,49,50$) at the data point (a_n) from a set of Raman intensities by correlating this data point to the reference regression line formed by the other 49 data points ($a_1, a_2, \ldots, a_{49}, a_{50}$, except the data point a_n). The value $C_{est,n}$ is compared with the corresponding reference concentration ($C_{ref,n}$) for each data point to calculate the root-mean-square error of estimation (RMSE),[12] $\mathrm{RMSE} = [(1/50)\sum_{n=1}^{50}(C_{est,n} - C_{ref,n})^2]^{1/2} = 5.1$ mM. An RMSE of

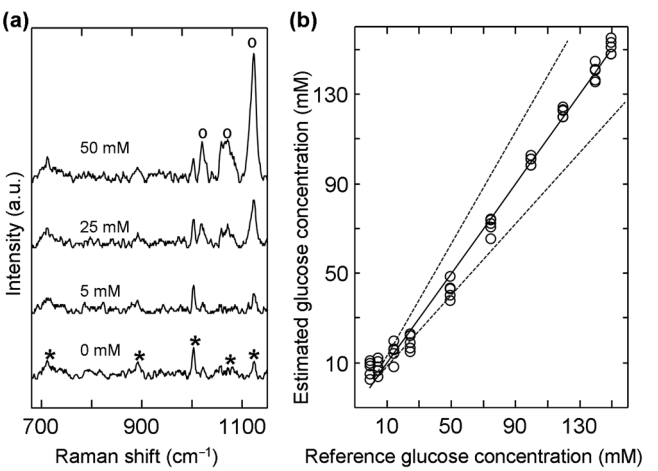

Fig. 5 (a) SERS spectra for the glucose concentrations of 0, 5, 25, and 50 mM positioned inside phantom at 760 μm below the surface measured by using the Ag-coated agarose microneedle at an excitation power of 5 mW. Asterisks and circles indicate the Raman peaks due to 1-decanethiol and glucose, respectively. (b) Relationship of the estimated glucose concentrations based on the PLS-LOO method from SERS spectra measured in phantom using the Ag-coated agarose microneedle to that of the reference glucose concentrations. Region within the two dotted lines demarcates the accuracy standard specified by the ISO/DIS 15197.

5.1 mM is obtained for the Ag-coated agarose microneedle (Fig. 5). This value is comparable with our SERS stainless steel microneedle with an RMSE of 3.3 mM[12] and other SERS sensors[15] with an RMSE range of 1.8 to 3 mM that were comprised of the Ag-coated polystyrene beads. The variation in the RMSE can be attributed to differences in the surface roughness of the Ag formed by the Tollen's method[12] in our technique and the vapor deposition reported in the literature.[15] In addition, the underlying agarose could have larger roughness than that of the stainless steel, which is probably reflected in the larger surface roughness for the Ag layer coated on the agarose than that of the stainless steel microneedle (Fig. 6). Among these methods, our SERS strategy allows *in situ* glucose measurements, although the RMSE is slightly larger. This strategy shows the detection of glucose concentrations ranging from 0 to 250 mM, which covers the clinical ranges[15] of glucose concentrations from hypoglycemia (2.8 mM or 50 mg/dl) to severe diabetes (72.2 mM or 1300 mg/dl) with an RMSE close to the clinically desirable value of 1 mM (18 mg/dl). Our strategy also shows the potential to meet the International Organization for Standardization, ISO/DIS 15197 standard[22] [demarcated by the region in Fig. 5(b) within the dotted region], which requires a sensor to be able to identify a difference of 0.8 mM (15 mg/dl) in the glucose level for a reference concentration less than 4.2 mM (75 mg/dl) and a difference of around 20% of the true value for a reference concentration more than 4.2 mM. The RMSE could be reduced with an improved repeatability and sensitivity in the SERS measurements by fabricating a more reproducible and sensitive SERS layer. The potential modification strategies to improve the repeatability include the surface roughness reduction of Ag nanoparticles and that of the agarose microneedle, prior to Ag coating, the size standardization of Ag nanoparticles, and the utilization of other SERS-active materials, e.g., gold. The strategies to improve the sensitivity include the realization of novel nanostructures, such as nanogaps, inside the nanoparticle film. Prior to the implementation of *in vivo* glucose measurements, we will measure the SERS spectra for the mixture of blood and glucose at known concentrations. With these acquired spectra, the PLS regression and a LOO analysis will be performed to calibrate the SERS intensities against the glucose concentrations in the mixture. Additionally, we will improve the entire probe design to prevent the blood from entering into the lumen, such as to implement a needle hub to fit the microneedle tightly to the objective. This design is equivalent to a hypodermic needle fixed to a syringe,[23] in which it is difficult to get blood into the lumen without pulling the plunger.

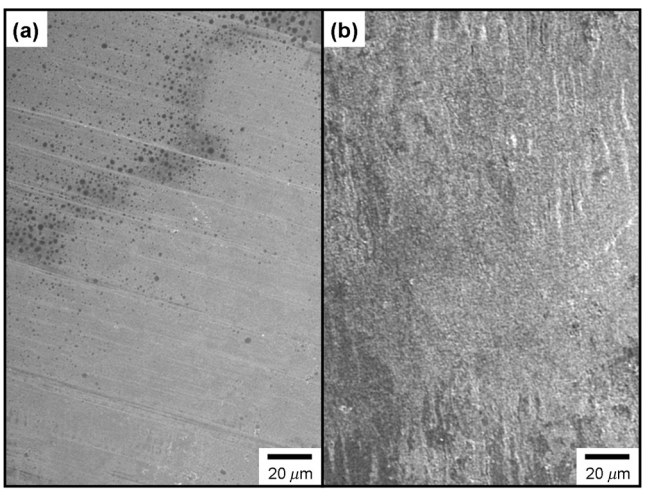

Fig. 6 Zoomed in FESEM images of (a) stainless steel microneedle and (b) agarose microneedle without silver coating.

3.4 *Shape-Changing Capability of Ag-Coated Agarose Microneedle*

We also characterize the microneedle shape-changing capability (Fig. 7). Figure 7(a) shows the Ag-coated agarose microneedle prior to insertion into the phantom. Upon insertion into the phantom, one portion of the microneedle swells inside the phantom, while the portion of the microneedle exposed to the air remains in its original size [Fig. 7(b)]. This size change of the agarose microneedle could be more clearly seen in Fig. 7(c) after the removal of the agarose microneedle from the phantom. Furthermore, permanent deformation of the agarose could be easily achieved by pressing the tip of the needle against a hard surface [Fig. 7(d)], which could prevent the recycled use of the needle. The size dependence of the agarose microneedle on the time it remains inside the skin phantom [Fig. 7(e)] is also investigated under a microscope. A $9\% \pm 2\%$ change in size is observed during the first 10 s, which is the time interval typically spent in a Raman measurement in this study. Moreover, a total size change of $53.9\% \pm 2\%$ is noted for each of the five different agarose microneedles after another additional 360 s inside the phantom. Additionally, the Ag-coated agarose microneedle is capable of piercing through the skin at different angles to the skin surface [Figs. 8(a) and 8(b)] and leaves clean-puncture edges at the penetration point [Fig. 8(c)]. After using these Ag-coated agarose microneedles, we could see that the tip of the microneedle is bent [Fig. 8(d)] in comparison with the microneedle before insertion [Fig. 3(a)].

This utilization of agarose as the microneedle material is advantageous for: (1) probing by exploiting the insoluble[24] characteristic of agarose in contrast to other microneedle materials,

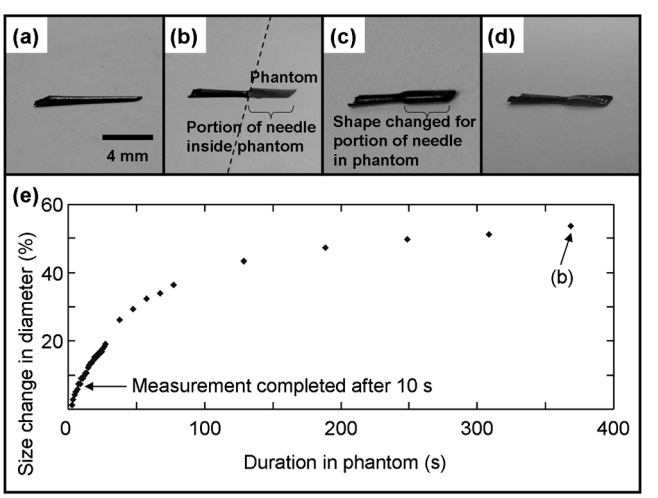

Fig. 7 Ag-coated agarose microneedle (a) before and (b) after insertion into phantom (defined by the dash line) for more than 6 min and (c) removed from phantom after insertion with (d) permanent deformation after pressing onto the tip area. (e) Size variation of agarose microneedle inside phantom as a function of time. At about 10 s, the SERS measurement is completed with a size change of about 9%, in contrast to the variation of 53.9% for another 6 min inside the phantom.

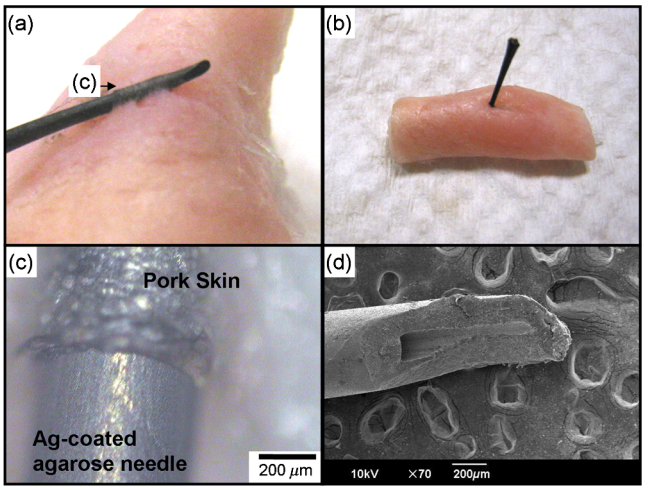

Fig. 8 Penetration of pig skin at an angle almost (a) parallel and (b) perpendicular. (c) Zoom in image of (a). (d) SEM image of an Ag-coated agarose microneedle with a blunt tip after insertion.

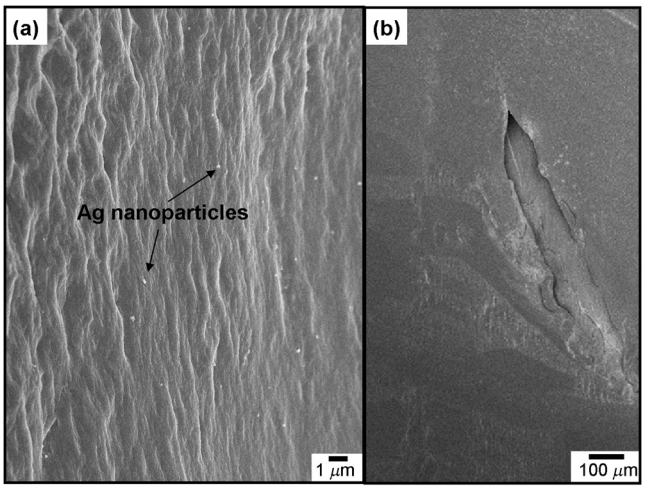

Fig. 9 FESEM (a) image and (b) zoomed-in image of cross-section of phantom after removing the inserted Ag-coated agarose microneedle.

such as polyvinylpyrrolidone,[1] which could be dissolved in the intradermal layer; (2) demonstration of effective penetration Fig. 8) to function as an intradermal measurement probe (Figs. 4 and 5) in addition to those functions reported in the literature[14] that could only show the mechanical interlocking of tissues and delivery of bioactive therapeutics by microneedles without lumens; and (3) prevention of sharp injuries and recycling use of these microneedles, since shape changing of this material could be effectively realized (Figs. 7 and 8) after prolonged soaking of the agarose microneedle in water. Contrarily, the agarose microneedle also has weaknesses which includes the accidental breakage of needles inside the human skin, which is similar to that of other metal[3,11–13] needles, but this potentially serious issue[25] could be minimized, since the material is agarose. Results in this study offer a guide for the future optimization of this strategy in geometries, thicknesses, structures, and types of the (1) SERS active layer and (2) microneedle materials, which intend to further enhance the mechanical strength, the SERS Raman signal, and the swelling characteristic of these agarose microneedles for measurements in the *in vivo* and *ex vivo* experiments. The need to develop this safe microneedle probe is pressing, since the injection[10] of SERS-active nanoparticles for Raman measurements can be toxic. These Ag nanoparticles could probably lead to argyria for exposure at level more than the permissible exposure limit of 0.01 mg/m^3 set by the US Occupational Safety and Health Administration.[26] Moreover, these nanoparticles can induce inflammation, cellular destruction, and genotoxicity into the different types of cell lines such as macrophages, fibroblasts, and embryonic stem cells in the cell culture study.[27] Prospective studies have to be performed for preventing detached nanoparticles from our microneedle being left behind in the cross-section of an agarose phantom taken by FESEM [Fig. 9(a)] after the Ag-coated agarose microneedle was removed from the phantom, as illustrated in the zoomed-in image of Fig. 9(b). Execution of this investigation and other toxicity tests is necessary prior to clinical studies and requires approval as a medical device by international health agencies (e.g., the silver-coated catheters and nanosilver dressing[28] approved by the Food and Drug Administration). This investigation is utilized to avoid the phagocytosis of nanoparticles by the vascular endothelial cells and the entry into the bloodstream, resulting in the accumulation[29] of nanoparticles in different organs such as the kidney, liver, and spleen. Nevertheless, the Ag-coated agarose microneedle is promising for use as a single use zero-sharp waste needle probe for intradermal SERS measurements to eliminate the subcutaneous injection of nanoparticles in the typical SERS *in vivo* measurements. This report also serves as the first observation for the agarose microneedle being used as a prospective probe for safe measurements.

4 Conclusion

In conclusion, we demonstrate a SERS agarose miconeedle used to achieve trace chemical analysis and quantification of test molecules, CV and glucose, embedded at a depth of more than 700 μm below the surface of a skin phantom. The nonreusability of the agarose microneedle and its size-changing capability that prevents sharp injury make our strategy promising for safe *in vivo* intradermal SERS measurements.

Appendix: Reason for the Microneedle to Be Coated with a Layer of 1-Decanethiol in the SERS Detection of Glucose by Using the Ag-Coated Microneedle

The use of this modifying molecular layer helped in the glucose quantification measurements and prevented the Ag coating from undergoing oxidation, which was reported in the literature for other types of Ag-coated substrates for glucose SERS measurements. 1-Decanethiol was used to coat the Ag-coated agarose microneedles for glucose detection, since this layer of 1-decanethiol molecules can capture glucose molecules in close vicinity to the Ag nanoparticles and increase its local concentration. The use of this modifying molecular layer helped the glucose quantification measurements and prevented the Ag coating from oxidation, which was reported in the literature for other types of Ag-coated substrates for glucose SERS measurements. Also, 1-decanethiol was employed because the thickness of this molecular layer was comparatively smaller than that formed by other modifying molecules,[15] such as 1-hexanethiol and 1-octanethiol. This feature would allow the glucose test molecules to be closer to the active Ag layer to yield stronger Raman

enhancement than other surface modifying layers, since the SERS signal decreases with the distance increment between the test molecules and the Ag layer.

Acknowledgments

The authors would like to acknowledge funding from the Lee Kuan Yew (LKY) start-up grant, the LKY research fellowship, ASTAR-ANR joint grant (Grant No. 102 167 0115) and the public sector funding grant (Grant No. 122-PSF-0012) funded by ASTAR-SERC (Agency for Science Technology and Research, Science and Engineering Research Council) in Singapore.

References

1. S. P. Sullivan et al., "Dissolving polymer microneedle patches for influenza vaccination," *Nat. Med.* **16**(8), 915–920 (2010).
2. C. G. Li et al., "An optimized hollow microneedle for minimally invasive blood extraction," *Biomed. Microdevices* **15**(1), 17–25 (2013).
3. M. A. Invernale et al., "Microneedle electrodes toward an amperometric glucose-sensing smart patch," *Adv. Healthcare Mater.* **3**(3), 338–342 (2014).
4. W. R. Health and F. R. Carbone, "Dendritic cell subsets in primary and secondary T cell responses at body surfaces," *Nat. Immunol.* **10**(12), 1237–1244 (2009).
5. T. Nakatsuji et al., "The microbiome extends to subepidermal compartments of normal skin," *Nat. Commun.* **4**, 1431 (2013); J. T. Whitton and J. D. Everall, "The thickness of the epidermis," *Br. J. Dermatol.* **89**(5), 467–476 (1973).
6. R. Bardhan et al., "Theranostic nanoshells: from probe design to imaging and treatment of cancer," *Acc. Chem. Res.* **44**(10), 936–946 (2011).
7. Y. H. Ong and Q. Liu, "Axicon lens-based cone shell configuration for depth-sensitive fluorescence measurement in turbid media," *Opt. Lett.* **38**(15), 2647–2649 (2013).
8. C. Krafft, B. Dietzek, and J. Popp, "Raman and CARS microspectroscopy of cells and tissues," *Analyst* **134**(6), 1046–1057 (2009).
9. C. Yuen and Q. Liu, "Magnetic field enriched surface enhanced resonance Raman spectroscopy for early malaria diagnosis," *J. Biomed. Opt.* **17**(1), 017005 (2012).
10. V. Amendola et al., "Magneto-plasmonic Au-Fe alloy nanoparticles designed for multimodal SERS-MRI-CT Imaging," *Small* **10**(12), 2476–2486 (2014).
11. J. Dong et al., "Minimally invasive surface-enhanced Raman scattering detection with depth profiles based on a surface-enhanced Raman scattering-active acupuncture needle," *Anal. Chem.* **83**(16), 6191–6195 (2011).
12. C. Yuen and Q. Liu, "Towards *in vivo* intradermal surface enhanced Raman scattering (SERS) measurements: silver coated microneedle SERS probe," *J. Biophotonics* **7**(9), 683–689 (2013).
13. M. M. Levine, "Can needle-free administration of vaccines become the norm in global immunization?," *Nat. Med.* **9**(1), 99–103 (2003).
14. S. Y. Yang et al., "A bio-inspired swellable microneedle adhesive for mechanical interlocking with tissue," *Nat. Commun.* **4**, 1702 (2013).
15. K. E. Shafer-Peltier et al., "Toward a glucose biosensor on surface-enhanced Raman scattering," *J. Am. Chem. Soc.* **125**(2), 588–593 (2003).
16. M. I. A. Joshy et al., "Freeze dried cross linking free biodegradable composites with microstructures for tissue engineering and drug delivery application," *Mater. Sci. Eng. C* **33**(1), 466–474 (2013).
17. V. Sachdeva and A. K. Banga, "Microneedles and their applications," *Recent Pat. Drug Delivery Formulation* **5**(2), 95–132 (2011).
18. L. S. Dimas et al., "Tough composites inspired by mineralized natural materials: computation, 3D printing, and testing," *Adv. Funct. Mater.* **23**(36), 4629–4638 (2013).
19. M. Volny et al., "Surface-enhanced Raman spectroscopy of soft-landed polyatomic ions and molecules," *Anal. Chem.* **79**(12), 4543–4551 (2007).
20. X. Jiang et al., "Silver nanoparticle aggregates on copper foil for reliable quantitative SERS analysis of polycyclic aromatic hydrocarbons with a portable Raman spectrometer," *Analyst* **137**(17), 3995–4000 (2012).
21. H. Falsig et al., "Trends in the catalytic CO oxidation activity of nanoparticles," *Angew. Chem. Int. Ed.* **47**(26), 4835–4839 (2008); Y. S. Li, X. Lin, and Y. Cao, "Using a sol-gel process for the fabrication of surface-enhanced Raman scattering active substrates," *Vib. Spectrosc.* **20**(1), 95–101 (1999).
22. K. Ma et al., "In vivo, transcutaneous glucose sensing using surface-enhanced spatially offset Raman spectroscopy: multiple rats, improved hypoglycemic accuracy, low incident power, and continuous monitoring for greater than 17 days," *Anal. Chem.* **83**(23), 9146–9152 (2011).
23. J. Donovan and P. Brown, "Parenteral injections," *Curr. Protoc. Immunol.* **73**, 1.6.1–1.6.10 (2006).
24. T. J. Trivedi et al., "Agarose processing in protic and mixed protic-aprotic ionic liquids: dissolution, regeneration and high conductivity, high strength ionogels," *Green Chem.* **14**(10), 2831–2839 (2012).
25. M. R. Prausnitz, "Microneedles for transdermal drug delivery," *Adv. Drug Delivery Rev.* **56**(5), 581–587 (2004).
26. P. L. Drake and K. J. Hazelwood, "Exposure-related health effects of silver and silver compounds: a review," *Ann. Occup. Hyg.* **49**(7), 575–585 (2005).
27. M. V. Park et al., "The effect of particle size on the cytotoxicity, inflammation, developmental toxicity and genotoxicity of silver nanoparticles," *Biomaterials* **32**(36), 9810–9817 (2011).
28. L. Ge et al., "Nanosilver particles in medical applications: synthesis, performance, and toxicity," *Int. J. Nanomed.* **9**(1), 2399–2407 (2014).
29. J. Tang et al., "Distribution, translocation and accumulation of silver nanoparticles in rats," *J. Nanosci. Nanotechnol.* **9**(8), 4924–4932 (2009).

Clement Yuen received the BEng and PhD degrees in electrical and electronics engineering (EEE) from Nanyang Technological University (NTU), Singapore, in 2002 and 2005, respectively. He was awarded with the graduate fellowship from the Agency for Science, Technology and Research, Singapore, during his PhD candidature. He was also awarded the Lee Kuan Yew postdoctoral fellowship and start-up grant, Singapore, for sponsoring his current research in SERS.

Quan Liu received a PhD degree in biomedical engineering from the University of Wisconsin, Madison, US. He is currently an assistant professor in the School of Chemical and Biomedical Engineering at Nanyang Technological University in Singapore. His research is focused on the development of optical imaging and spectroscopy techniques for medical diagnostics. He is a senior member of SPIE and a member of OSA.